

# Nonequilibrium Dynamics of the Chiral Phase Transition in Heavy Ion Collisions

---

**Kerstin Paech**<sup>\*†</sup>

*Michigan State University*

*E-mail: paech@msu.edu*

We study the hydrodynamical expansion of a hot and baryon-dense quark fluid coupled to classical real-time evolution of the long wavelength modes of the chiral field. We show that this process of chiral symmetry breaking in a real-time first-order phase transition can lead to large inhomogeneities of the baryon density in heavy-ion collisions. We find that the amplitude of the density inhomogeneities is larger for expansion trajectories crossing the line of first-order transitions than for crossovers, which could provide some information on the location of a critical point.

*The 3rd edition of the International Workshop — The Critical Point and Onset of Deconfinement —*

*July 3-7 2006*

*Galileo Galilei Institute, Florence, Italy*

---

<sup>\*</sup>Speaker.

<sup>†</sup>Feodor Lynen Fellow of the Alexander von Humboldt Foundation

## 1. Introduction

Relativistic heavy ion collisions are used to produce matter at high temperature and baryon density. The goal is to extract information about the transition that takes place between the hadronic (chirally broken) matter at low temperatures and densities and the deconfined (and approximately chirally symmetric) phase at high temperatures and/or densities. Lattice Gauge Theory [1] suggests that at sufficiently large baryon density a line of first order transitions exists in the plane of temperature  $T$  versus baryon-chemical potential  $\mu_B$  which separates those phases. Moving to lower baryon density (and higher temperature) on this phase boundary weakens the first order transition, and finally the line of first order phase transitions ends at a second order critical point [2] at  $T_{\text{crit}}$  and  $\mu_{\text{crit}}$ . Towards even lower baryon densities the two phases are continuously connected by a rapid crossover.

As a motivation for our studies we turn to the data taken on the temperature fluctuations of the cosmic microwave background (CMB) [3] taken by the WMAP collaboration. The background photons exhibit temperature fluctuations on the order of  $\Delta T/T \simeq 10^{-5}$ . From the CMB multipoles cosmologists hope to gather information on their primordial origin. We may use this idea to obtain information about the QCD phase transition. If a phase transition occurs in a heavy ion collision it might leave imprints on the (energy-) density distribution on the freeze-out hypersurface.

In the following we want to analyze the homogeneity of the “fluid” of QCD matter as it expands and cools. Being more specific, we will study the expansion trajectories passing on either side of the critical point, i.e. either crossover or first order transitions. We will show that in the vicinity of the critical point the expanding fluid develops significant inhomogeneities. These density perturbations should also be present on the decoupling surface of hadrons.

## 2. Chiral Hydrodynamics

Chiral Hydrodynamics [4, 5] assumes that the long-wavelength (classical) modes of the chiral fields evolve in the effective potential generated by the thermalized degrees of freedom, which are the matter fields (and possibly also hard modes of the chiral field, i.e.  $\sigma$  and  $\vec{\pi}$  particles, which are however neglected here for simplicity). In our model, the latter are described as a perfect relativistic fluid, whose equation of state is in turn determined by the chiral field (via the effective mass), and which can exchange energy and momentum with the chiral fields. The chiral symmetry breaking dynamics is described by an effective field theory, in our case the  $SU(2) \times SU(2)$  linear  $\sigma$ -model:

$$\mathcal{L} = \bar{q} [i\gamma^\mu \partial_\mu - g(\sigma + i\gamma_5 \vec{\tau} \cdot \vec{\pi})] q + \frac{1}{2} (\partial_\mu \sigma \partial^\mu \sigma + \partial_\mu \vec{\pi} \partial^\mu \vec{\pi}) - U(\sigma, \vec{\pi}) \quad . \quad (2.1)$$

The potential  $U(\sigma, \vec{\pi})$ , which exhibits both spontaneously and explicitly broken symmetry, is given by

$$U(\sigma, \vec{\pi}) = \frac{\lambda^2}{4} (\sigma^2 + \vec{\pi}^2 - v^2)^2 - h_q \sigma \quad . \quad (2.2)$$

Here  $q$  is the constituent-quark field  $q = (u, d)$ . The scalar field  $\sigma$  and the pseudoscalar field  $\vec{\pi}$  together form a chiral field  $\phi = (\sigma, \vec{\pi})$ . The vacuum expectation values of the condensates are  $\langle \sigma \rangle = f_\pi$  and  $\langle \vec{\pi} \rangle = 0$ , where  $f_\pi = 93$  MeV is the pion decay constant.

For  $g > 0$ , the finite-temperature one-loop effective potential includes a contribution from the quarks, and is given by

$$V_{\text{eff}}(\phi, T) = U(\phi) - d_q \int \frac{d^3 \vec{p}}{(2\pi)^3} T \left\{ \log \left( 1 + e^{(\mu - E)/T} \right) + (\mu \rightarrow -\mu) \right\} \quad (2.3)$$

$V_{\text{eff}}$  depends on the order parameter field through the effective mass of the quarks,  $m_q = g|\phi|$ , which enters the expression for the energy  $E$ .

For sufficiently small quark-chemical potential  $\mu$  one finds a smooth transition to approximately massless quarks at high  $T$ . For larger chemical potential, however, the effective potential exhibits a first-order phase transition [6]. Along the line of first-order transitions the effective potential exhibits two degenerate minima which are separated by a “nucleation barrier”. This barrier decreases with  $\mu$  and the two minima approach each other. At  $\mu_E$ , finally, the barrier vanishes, and so does the latent heat. For  $g = 3.3$ , which leads to a constituent quark mass in vacuum of  $\approx 307$  MeV, the second-order critical point is located at  $T_E \approx 100$  MeV,  $\mu_E \approx 200$  MeV. Increasing the quark-field coupling  $g$  moves the endpoint  $E$  towards the temperature axis [7] ( $\mu_E$  becomes  $=0$  at about  $g \approx 3.7$  [5]) and to slightly higher temperature. In what follows, we fix  $g = 3.3$ .

The classical equations of motion for the chiral fields are

$$\partial_\mu \partial^\mu \phi + \frac{\delta V_{\text{eff}}}{\delta \phi} = 0 \quad (2.4)$$

The dynamical evolution of the thermalized degrees of freedom (fluid of quarks) is determined by the local conservation laws for energy and momentum. Note that we do not assume that the chiral fields are in equilibrium with the heat bath of quarks. Hence, the fluid pressure  $p$  depends explicitly on  $|\phi|$ , see [5] for more details. Due to the interaction between fluid and field the *total* energy and momentum is the conserved quantity:

$$\partial_\mu \left( T_{\text{fluid}}^{\mu\nu} + T_\phi^{\mu\nu} \right) = 0. \quad (2.5)$$

We emphasize that we employ eq. (2.4) not only to propagate the mean field through the transition but fluctuations as well. The initial condition includes some generic “primordial” spectrum of fluctuations (see below) which then evolve in the effective potential generated by the matter fields. The presence of these fluctuations affects the relaxation rate of the zero-mode of the field via “nucleation” or “spinodal decomposition” to the new ground state, see e.g. the discussion in [8].

### 3. Results

#### 3.1 Initial Conditions

Our goal is to get a qualitative understanding of the out of equilibrium dynamics of a system undergoing a transition from the chirally restored to the chirally broken phase. Therefore we choose the following simple set of initial conditions. We start with a sphere of hot and dense quarks with radius  $R = 5$  fm and no initial collective motion,  $\vec{v}(t = 0) = 0$ . The average chiral field within the sphere corresponds to the minimum of the effective potential  $V_{\text{eff}}$  at some given energy and baryon

density. The system subsequently expands hydrodynamically on account of the nonzero pressure. We choose

$$\begin{aligned} e(t=0, \vec{x}) &= \frac{e_{\text{eq}}}{1 + \exp\left(\frac{r-R}{a}\right)} & \sigma(t=0, \vec{x}) &= \delta\sigma(\vec{x}) + f_\pi + \frac{\sigma_{\text{eq}} - f_\pi}{1 + \exp\left(\frac{r-R}{a}\right)} \\ \rho(t=0, \vec{x}) &= \frac{\rho_{\text{eq}}}{1 + \exp\left(\frac{r-R}{a}\right)} & \vec{\pi}(t=0, \vec{x}) &= \delta\vec{\pi}, \end{aligned} \quad (3.1)$$

with  $a = 0.3$  fm the surface thickness of the initial density distribution. Here  $\sigma_{\text{eq}} \approx 0$  is the value of the  $\sigma$  field corresponding to  $e_{\text{eq}}$  and  $\rho_{\text{eq}}$ .  $\delta\sigma(\vec{x})$  represents Gaussian random fluctuations of the fields which are distributed according to

$$P[\delta\phi_a] \propto \exp\left(-\delta\phi_a^2/2\langle\delta\phi_a^2\rangle\right). \quad (3.2)$$

The results presented here were obtained with a width of  $\sqrt{\langle\delta\sigma^2\rangle} = v/3$ ,  $\sqrt{\langle\delta\vec{\pi}^2\rangle} = 0$ .

These relatively moderate amplitudes suffice to probe the structure of the effective potential near the transition. Larger fluctuations would amplify the effects shown below. The initial field fluctuations are initially correlated over approximately 1 fm as described in [5]. Our focus is on how those ‘‘primordial’’ fluctuations evolve through the various transitions.

We will apply two different sets of initial conditions: for set (I) we start the evolution at fixed initial energy density  $e_{\text{eq}} = 2.8e_0$  but vary the initial baryon density  $\rho_{\text{eq}} = (0, 0.6, 1.6, 2.1, 2.4, 2.8)\rho_0$ ; for set (II), on the other hand, we start at fixed initial net baryon density  $\rho_{\text{eq}} = 1.7\rho_0$  but vary the initial energy density  $e_{\text{eq}} = (1.4, 1.9, 2.9)e_0$ . Here,  $e_0$  and  $\rho_0$  denote nuclear matter ground state energy and baryon density, respectively. For low baryon density (I) (high energy density (II)), the expansion will then proceed through a crossover, while a baryon dense (I) (energy dilute (II)) droplet will decay via a first-order phase transition.

### 3.2 Time evolution

Fig. 1 shows the trajectory of the average energy and baryon density within the phase diagram for both sets of initial conditions (see [9] for details). Initial conditions with  $\mu_0 < \mu_{\text{crit}}$  correspond to a smooth evolution via a crossover. For all other initial conditions, the system evolves through the region corresponding to phase coexistence in the equilibrium phase diagram and undergoes a first order phase transition. The initial Gaussian field fluctuations (3.2) which propagate through the phase transition induce fluctuations of the fluid density  $\Delta\rho$  [9].

The time evolution of the baryon density inhomogeneities for initial condition set (I) is shown in fig. 2 as a function of the average baryon density of the system. For this set of initial conditions we start at the same initial energy density, but different initial baryon density. Further, we start with fluctuations of the order parameter field only, so that initially  $\Delta e = \Delta\rho = 0$ ; this is to show the minimal degree of inhomogeneity induced just by the transition to the symmetry broken state. As the evolution progresses, the fluctuations of the order parameter field rapidly lead to density inhomogeneities in the quark fluid. At the same time the system expands and the density decreases, therefore later time steps correspond to lower baryon densities. One observes that the baryon density inhomogeneities are sensitive to the dynamical evolution.

For large initial baryon density the expansion proceeds through the region of first-order phase transitions. Here, the effective potential exhibits two local minima within the ‘‘phase coexistence’’

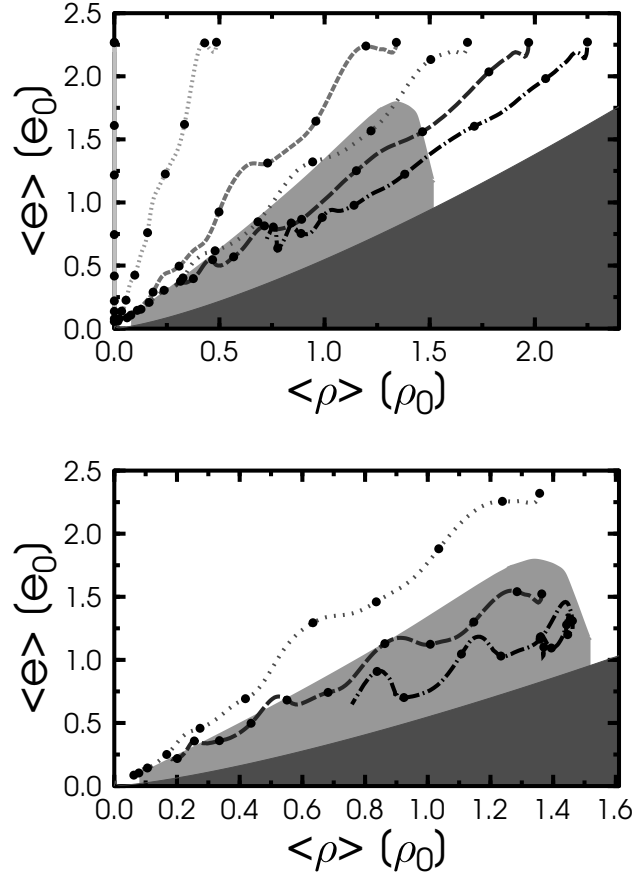


**Figure 1:** Evolution of the average fluid energy and baryon density through a crossover, and a weak and strong first order transition, respectively, for initial conditions I (top) and II (bottom). The densities are measured in units of nuclear matter saturation density  $\rho_0 \approx 0.16 \text{ fm}^{-3}$ ,  $e_0 = m_N \rho_0 \approx 0.15 \text{ GeV/fm}^3$ , with  $m_N \approx 0.922 \text{ GeV}$  the mass of a nucleon bound in infinite matter. The fat dots indicate time intervals of  $\approx 1.5 \text{ fm/c}$ . The phase coexistence region is shaded in grey.

region of the equilibrium phase diagram (see e.g. fig. 1 in [5] or figs. 2-4 in [6]) and so in some region of space the order parameter can be “trapped” in the symmetric phase until reaching the spinodal instability [10]. This effect is more pronounced the stronger the first-order phase transition, i.e. the smaller the entropy per baryon. Consequently, density perturbations can only wash out after the double-minimum structure of the effective potential has disappeared and the order parameter “rolls down” to its new vacuum. There is therefore reasonable hope that these inhomogeneities created during the non-equilibrium phase transition are present in the final state, contrary to those from the initial state. However, even for a crossover substantial inhomogeneities could be present in the final state if they “freeze” shortly after passing the point where  $V_{\text{eff}}$  is flattest (or where the chiral susceptibility  $\partial^2 V_{\text{eff}} / \partial \sigma^2$  peaks, respectively).

To make sure that the different behavior of the density inhomogeneities for the set (I) of initial conditions is not an effect of the different initial baryon densities we turn to the second set of initial conditions (II). Here we start at the same initial baryon density, but different initial energy density.

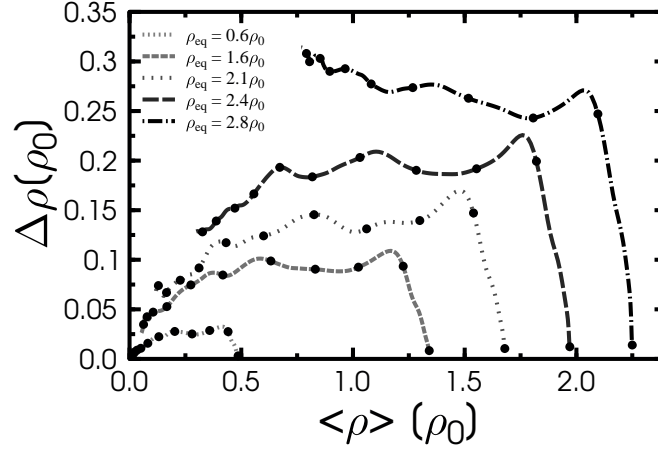


**Figure 2:** RMS fluctuations of the baryon density with initial condition set (I) for crossover (narrow-dots, short-dashes), weak (wide-dots, long-dashes) and strong (dash-dots) first order transitions as a function of the average baryon density. The fat dots indicate time intervals of  $\approx 1.5$  fm/c.

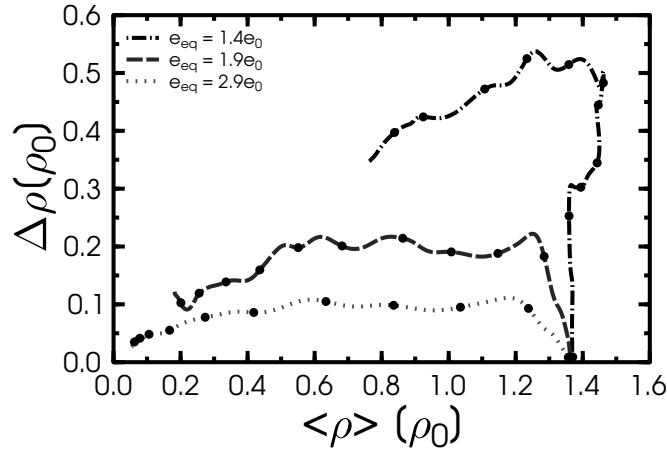


**Figure 3:** RMS fluctuations of the baryon density with initial condition set (II) for crossover (dots), weak (dashes) and strong (dash-dots) first order transition as a function of the average baryon density. The fat dots indicate time intervals of  $\approx 1.5$  fm/c.

Fig 3 shows results for the set (II) of initial conditions, corresponding to *fixed* initial baryon density  $\rho_{\text{eq}} = 1.7\rho_0$  but *different* initial energy density  $e_{\text{eq}}$ . Again, the amplitude of the density contrast is substantially larger for a strong first order transition ( $e_{\text{eq}} = 1.4e_0$ ) than for a crossover ( $e_{\text{eq}} = 2.9e_0$ ).

#### 4. Conclusion

The non-equilibrium dynamics of the order parameter field in heavy ion collisions can lead to large density inhomogeneities on the order of  $\Delta\rho/\rho_0 \sim 0.1 - 1$ . Also, the amplitude of the

fluctuations depends on the structure of the effective potential: the effect is stronger for a first-order phase transition than for a crossover.

So far we have not explored the possible experimental signatures that could arise. In analogy to inhomogeneous Big Bang nucleosynthesis [11] one might expect that the relative hadron abundances in heavy ion collisions are modified. This is because the densities of various hadron species depend non-linearly on the local energy and baryon density of the hadron fluid. This could be studied, for example, in the following simple model for an inhomogeneous decoupling surface as was discussed in [13]. Other observables should also exhibit some sensitivity to inhomogeneities, e.g. Hanbury-Brown–Twiss correlations for pions [14] or production cross sections for light (anti-) nuclei, formed by coalescence of (anti-) nucleons.

## Acknowledgments

I thank Adrian Dumitru for his collaboration in the past. I gratefully acknowledge support from the by the Alexander-von-Humboldt foundation.

## References

- [1] Z. Fodor and S. D. Katz, JHEP **0404** (2004) 050.
- [2] M. Stephanov, K. Rajagopal and E. V. Shuryak, Phys. Rev. Lett. **81**, (1998) 4816.
- [3] C.L. Bennett et al., ApJS **148** (2003) 1; H.V. Peiris et al., ApJS **148** (2003) 213.
- [4] I. N. Mishustin, J. A. Pedersen and O. Scavenius Heavy Ion Phys. **5** (1997) 377
- [5] K. Paech, H. Stocker and A. Dumitru nucl-th/0302013
- [6] O. Scavenius, A. Mocsy, I. N. Mishustin and D. H. Rischke, Phys. Rev. C **64** (2001) 045202.
- [7] O. Scavenius et al., Phys. Rev. Lett. **83** (1999) 4697; Phys. Rev. D **63** (2001) 116003.
- [8] B. G. Taketani and E. S. Fraga, arXiv:hep-ph/0604036.
- [9] K. Paech and A. Dumitru, Phys. Lett. B **623**, 200 (2005)
- [10] O. Scavenius *et al.*, Phys. Rev. Lett. **83** (1999) 4697; Phys. Rev. D **63** (2001) 116003
- [11] J. H. Applegate, C. J. Hogan and R. J. Scherrer, Phys. Rev. D **35** (1987) 1151; G. M. Fuller, G. J. Mathews and C. R. Alcock, Phys. Rev. D **37** (1988) 1380; K. Kainulainen, H. Kurki-Suonio and E. Sihvola, Phys. Rev. D **59** (1999) 083505.
- [12] for a review see P. Braun-Munzinger, K. Redlich and J. Stachel, arXiv:nucl-th/0304013 and references therein.
- [13] A. Dumitru, L. Portugal and D. Zschiesche, Phys. Rev. C **73**, 024902 (2006)
- [14] O. J. Socolowski, F. Grassi, Y. Hama and T. Kodama, Phys. Rev. Lett. **93** (2004) 182301.